Journal of Alloys and Compounds 489 (2010) 389–393

Contents lists available at ScienceDirect

Journal of Alloys and Compounds

journal homepage: www.elsevier.com/locate/jallcom

The novel eutectic microstructures of Si–Mn–P ternary alloy

Yaping Wu, Xiangfa Liu*

Key Laboratory for Liquid-Solid Structural Evolution and Processing of Materials, Ministry of Education, Shandong University, Jinan 250061, Shandong, PR China

ARTICLE INFO

Article history:
Received 26 August 2009
Received in revised form
18 September 2009
Accepted 19 September 2009
Available online 25 September 2009

Keywords:
Multicomponent alloy
Si–Mn–P master alloy
Eutectic
Solidification behavior

ABSTRACT

The microstructures of Si–Mn–P alloy manufactured by the technique of combining phosphorus transportation and alloy melting were investigated using electron probe micro-analyzer (EPMA). The phase compositions were determined by energy spectrum and the varieties of eutectic morphologies were discussed. It is found that there is no ternary compound but Si, MnP and $MnSi_{1.75-x}$ could appear when the Si–Mn–P alloy's composition is proper. Microstructure is greatly refined by rapid solidification technique and the amount of eutectic phases change with faster cooling rates. Moreover, primary Si or MnP are surrounded firstly by the binary eutectic (Si + MnP) and then the ternary eutectic (Si + $MnSi_{1.75-x}$ + MnP) which also exhibit binary structures due to divorced eutectic determined by the particularity of some Si–Mn–P alloys.

1. Introduction

The master alloys containing phosphorus such as Al–P or Al–Si–P applied to refine the primary Si in the hypereutectic Al–Si show good application prospect [1,2]. New master alloy Si–P also has a good modification effect on hypereutectic Al–Si alloys [3]. Some other elements are usually added into Si–P to make ternary alloy for promoting the dissolution of Si–P in Al–Si melt, for example, Si–Mn–P master alloys used in the production are commonly manufactured.

However, the Si–Mn–P alloy belongs to multicomponent alloy, whose properties are determined by the microstructures developing during solidification. The understanding and control of solidification microstructures are investigated in both practical and theory [4]. Much more attentions are paid to binary alloys rather than ternary alloys due to their complexity [5–6]. While in many commercial materials and industrial processes, ternary and multicomponent alloys are commonly used, therefore many researchers begin to dedicate to the multiphase solidification of ternary alloys [7–9]. The solidification microstructures of ternary alloys are complex involving binary eutectic, ternary eutectic or peritectic structures [10–11] and so on. Those alloys with the eutectic composition have many good properties, such as good fluidity, less dispersed shrinkage and hot cracking tendency [12]. Therefore, the microstructure of Si–Mn–P needs to be investigated in order to obtain better application.

Possible phases and interaction of components in the Co–Si–P, Re–Si–P, Mn–MnP–Si and W–Si–P alloys which involve the elements Si and P were discussed through synthesis of ternary alloys and research into corresponding binary systems [13–16]. However, the microstructure of Si–Mn–P was never reported before. In this paper, the microstructure of Si–15Mn–9P widely used in production is discussed. Si–43Mn–26P is manufactured according to the binary eutectic composition detected in Si–15Mn–9P for studying the eutectic. Si–20Mn–9P is also prepared to study the microstructure at higher cooling rates. Meanwhile, part of the solidification behavior of Si–Mn–P is presumed.

2. Materials and methods

Commercial pure crystalline Si (99.9%, all compositions quoted in this work are in wt.% unless otherwise stated), red phosphorus (99.9%), electrolytic Mn (99.9%) were used as raw materials to prepare Si–Mn–P alloys. Silicon and manganese alloys were firstly melted in high-temperature melting furnace. Homothermal phosphorous vapor was transported into the molten metals. After holding some proper time, the melt was poured to obtain an ingot [17].

The microstructure analysis was carried out on as-cast samples to investigate the morphology of the eutectic structure. Metallographic specimens were cut from the ingots at the same position and mechanically ground using standard routines. Then the microstructures were analyzed by using electron probe micro-analyzer (EPMA) (model JXA-8840, Japan).

3. Results and discussions

3.1. The as-cast microstructure and constituent phases of Si–15Mn–9P alloy

It is found that the microstructure of Si–Mn–P alloy is very unique when the ratio of constituents is proper. Fig. 1 shows

* Corresponding author. Tel.: +86 531 88392006; fax: +86 531 88395414.
E-mail address: xfliu@sdu.edu.cn (X. Liu).

0925-8388/$ – see front matter © 2009 Elsevier B.V. All rights reserved.
doi:10.1016/j.jallcom.2009.09.121

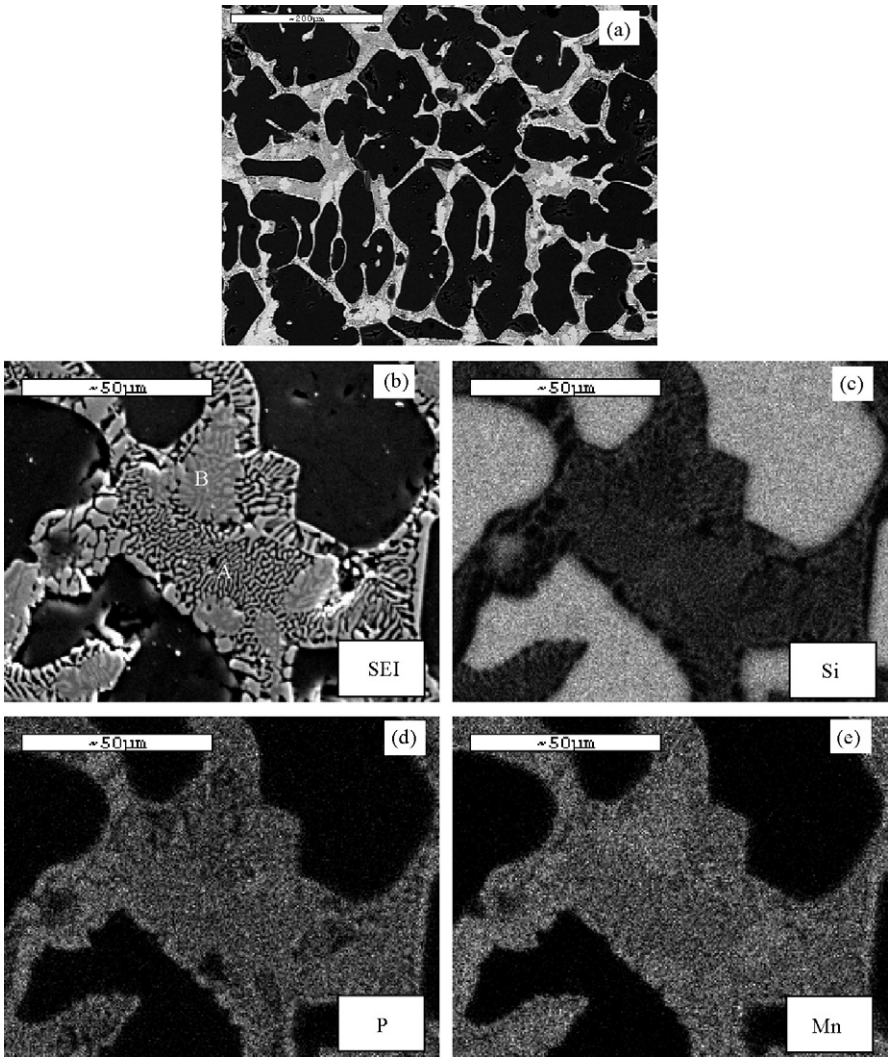

Fig. 1. Microstructure (a) and EPMA analysis of Si–15Mn–9P alloy; (b) SEI; (c–e) the X-ray images for respective elements: Si, P and Mn.

the microstructure and the EPMA analysis of Si–15Mn–9P. It can be seen obviously that there are two solidified eutectic microstructures (marked as A and B) with different morphology and composition besides the primary Si phase. By using the energy spectrum analysis, the stoichiometry of each phase was detected and listed in Table 1 below. Therefore, it can be deduced that the eutectic structure marked A is made up of two obvious phases, which are Si (the dark phase) and MnP (the light phase) respectively. The deep color phase of the eutectic structure marked B contains mainly silicon and manganese. The atomic ratio of silicon to manganese of this phase is nearly 1.72, and it is called higher manganese silicides (HMS) which have a composition of $MnSi_x$ with x ranging from 1.67 to 1.75. The subcells are nearly equal for all HMS with changing the translational symmetry of Si positions in the c-axis direction [18,19]. The main elements in the shallow color phase of the eutectic structure marked B are manganese and phosphorous, it is considered to be MnP compound according to the atomic ratio since the max number of phases in one ternary system is no more than four [20].

Table 1
The stoichiometry of each phase marked in Fig. 1 by using the energy spectrum analysis.

Phase	Elements contents (wt.%)		
	Si	Mn	P
Dark color phase in B	45.58	51.93	2.49
Light color phase in B	3.91	63.8	32.28
Light color phase in A	0.00	63.95	36.05
Dark color phase in A	97.28	1.09	1.63

It is found that the morphology of two eutectic structures varies besides the constituents. The variations for eutectic structure A (represents (Si + MnP) in this work unless otherwise stated) are more than B (represents the other eutectic in this work unless otherwise stated). Fig. 2 shows the different morphologies of the eutectic structure A, such as lamellar growth, labyrinth structures, sometimes island bonding and spherical eutectic morphology. However, in different eutectic cells, the varieties of morphologies may be attributed to different growing directions. For instance, the labyrinth structures in eutectic cell marked C may be taken as labyrinth structures in eutectic cell marked D with changing a direction, seen from Fig. 2. While in one independent eutectic cell, it can be seen that the primary phase is usually surrounded by the lamellar eutectic, which exhibits oscillatory behavior and finally evolves to be a labyrinth structure. The lamellar structure, labyrinth structure and spherical morphology all belong to the coupled growth. It is known that the coupled growth is stable only at a limited range of spacing and eutectic temperature [21]. The un-coupled growth will be developed if the dendrite arm spacing and eutectic temperature is out of this stable range, for example the island bonding mani-

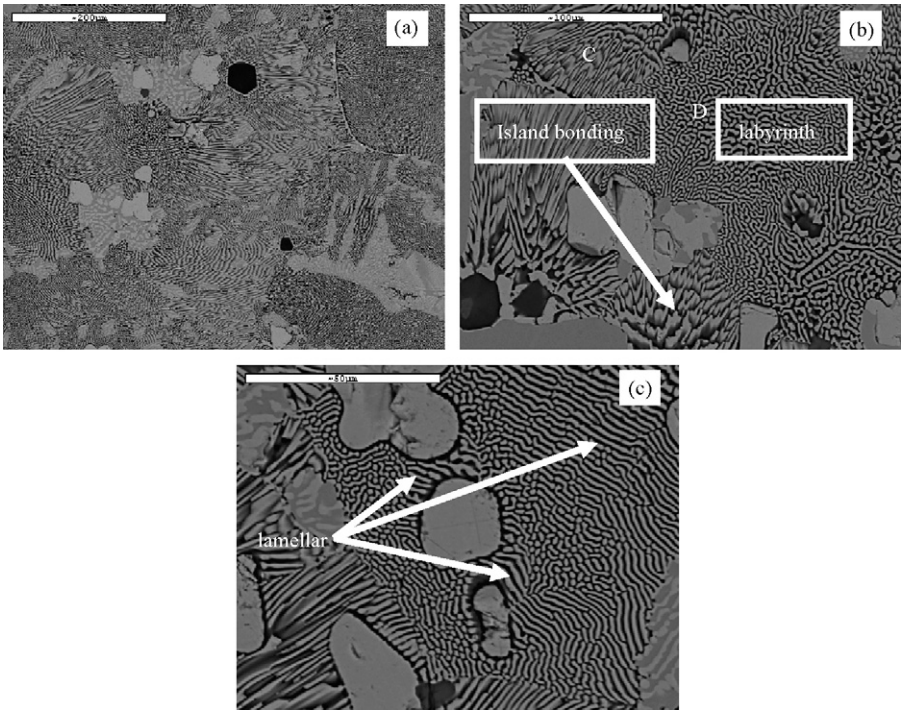

Fig. 2. Different morphologies of the eutectic Si + MnP structure: (a) low magnification; (b) middle magnification; (c) high magnification.

fested as the spreading of Si phase on MnP can also be observed in Fig. 2(b). The island bonding structure has been observed in directionally solidified binary peritectic Fe–Ni alloys which related the initiation of coupled growth from the island banding [22]. The lamellar eutectic growth is also unstable in the form of zigzag instability which can lead to the labyrinth structures depended on the initial spacing and the volume fractions [23].

The variations for the morphology of eutectic A are due to the complexity of binary eutectic in ternary alloys. In ternary alloys, growth of two solid phases from the liquid is no longer at a certain temperature the same as the binary alloys which can be interpreted according to the following phase rule when the pressure is constant [24]:

$$f = N - \phi + 1 \quad (1)$$

where N represents independent component number, ϕ represents phase number and f is the freedom degree.

The freedom degree reflects the factors which can change independently. Here during the formation of binary eutectics, both N and ϕ are to be 3, thus f is 1, which means that only the factor of temperature could change. The eutectic transformation from one liquid to two solid phases can go along in a temperature range owing to the addition of third element. The eutectic composition will change with the temperature. The shift of the eutectic composition caused by the change of eutectic temperature makes the growth conditions more complicated, thus multiple morphologies occur because of the instability of each kind of eutectic structure depended on associated critical spacing and growth conditions [23].

3.2. The microstructure of rapidly solidified Si–Mn–P alloys

It is known that higher cooling rates and shorter solidification time could lead to a more refined microstructure and extended solubility [25–26]. The rapidly solidified Si–20Mn–9P alloys were fabricated in order to investigate the evolution of microstructure with higher cooling rates. The microstructures of common and rapidly solidified Si–20Mn–9P are shown in Fig. 3. It is revealed that both the primary and eutectic phases are greatly refined through rapidly cooling. The relationship between the average lamellar spacing λ and undercooling ΔT in binary system is demonstrated by the JH model [27]:

$$\lambda \Delta T = c \quad (2)$$

where c is a constant number. However, the relationship becomes more complicated in the ternary system. The rule which λ and ΔT obey in ternary system is similar to that in binary system, though there are some factors related to ΔT [7]. In addition, the amount of eutectic B is increased in the rapidly solidified Si–20Mn–9P alloy, as seen from Fig. 3(b). The growth of primary phase and eutectic A could be inhibited due to the rapid solidification, so transformation into eutectic B initiates before much liquid has not solidified to be the primary phase or eutectic A yet. Therefore, it can also conclude that the eutectic B precipitates after A.

3.3. The solidification behavior of Si–Mn–P alloys

Fig. 4(a) presents the microstructure of Si–15Mn–9P alloys. It can be seen that the primary Si phase is firstly surrounded by the eutectic structure A among which distributes the eutectic structure B. Although Si–43Mn–26P alloy is prepared according to the composition of eutectic A, primary phase and the eutectic B occur more or less. It is well known that eutectics do not necessarily grow with the eutectic composition. The eutectic point could be shifted owing to nonequilibrium in the solidification process [28]. The microstructure of Si–43Mn–26P is indicated in Fig. 4(b), it shows that there are small amount of the primary phase and the eutectic structure B besides the majority of eutectic structure A. As different from Si–15Mn–9P alloy, the primary phase of Si–43Mn–26P is MnP which is surrounded by eutectic structure A. The amount of the eutectic structure B appears much less than that of Si–15Mn–9P.

Neither of the two eutectic structures is obtained by the quasiperitectic reaction according to their phase constituents. The

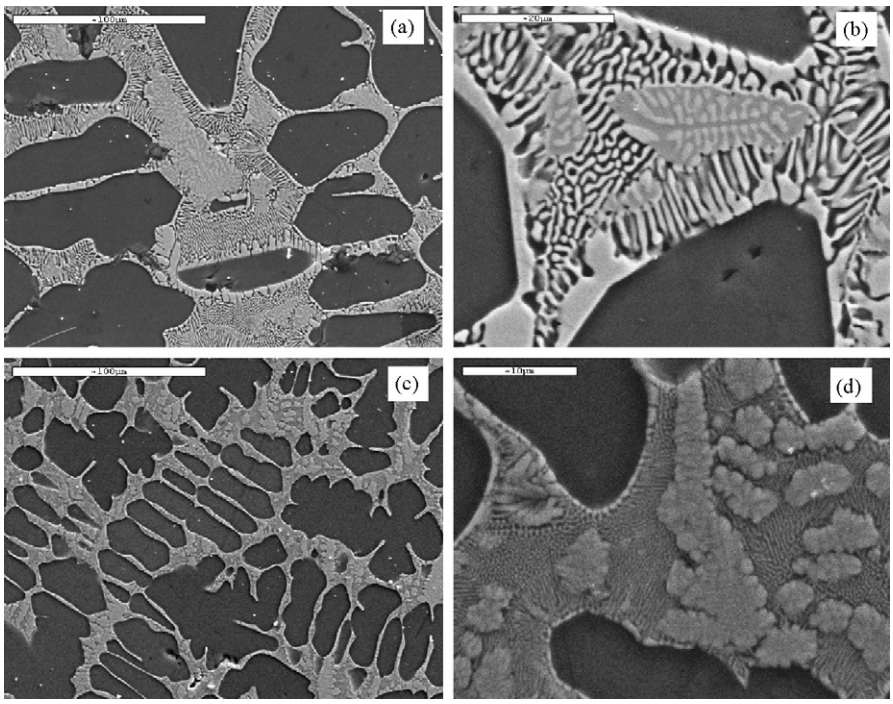

Fig. 3. The microstructures of common Si–20Mn–9P at low magnification (a); high magnification (b); and rapidly solidified Si–20Mn–9P at low magnification (c); high magnification (d).

eutectic structure B which distributes among A appears to be constructed by two phases. However, it does not conform to the adjacent rule of phase region for two kinds of binary solid phases growing from the liquid continuously. According to the phase boundary theory [29]:

$$R_1' = R_1 + \psi_c \tag{3}$$

$$R_1 = N + 1 - \psi \tag{4}$$

where R_1' is the geometric boundary dimension of two adjacent phase regions. R_1 is the dimension of phase boundary. ψ_c is the number of phases which are the same in the two neighboring phase regions. N is the independent component number. ψ is the total number of the two adjacent phase regions.

If the eutectic B belongs to binary eutectic the same as A, which means the adjacent phase region in the solidifying process is (L + Si + MnP)/(L + $MnSi_{1.75-x}$ + MnP), then here ψ, ψ_c can be gotten as 4, 2 respectively. Thus R_1 and R_1' is calculated as 0 and 2, which signify the boundary for adjacent phase region (L + Si + MnP)/(L + $MnSi_{1.75-x}$ + MnP) is a horizontal plane in which four phases (L, Si, MnP, $MnSi_{1.75-x}$) coexist. It is contradictory for liquid in (L + $MnSi_{1.75-x}$ + MnP) phase region exists below the four-phase coexisting plane. Therefore it can be concluded that the eutectic structure B distributes among the eutectic A is not generated by the binary eutectic reaction.

In the Si–Mn–P ternary system, it is known that the lines between composition points of $MnSi_{1.75-x}$, Si and MnP divide the concentration triangle of Si–Mn–P into three parts, as shown in Fig. 5. Therefore we can study the phase region separately to simplify the entire ternary system. Here the attention is focused on the $MnSi_{1.75-x}$–Si–MnP ternary system in which the usual composition of Si–Mn–P alloy locates. From the Mn–Si phase diagram, the eutectic structure of ($MnSi_{1.75-x}$ + Si) can be obtained when the atom percent of silicon reaches 63.4% [30]. However, the eutectic point is very near the $MnSi_{1.75-x}$ side. It means that the amount of Si phase is little in this eutectic structure. So in the $MnSi_{1.75-x}$–Si–MnP ternary system, the ternary eutectic point is far away from the pure component Si which signifies the amount of Si phase in the ternary eutectic is also little. Consequently during the formation of eutectic B, the little amount of Si phase can grow in adherence

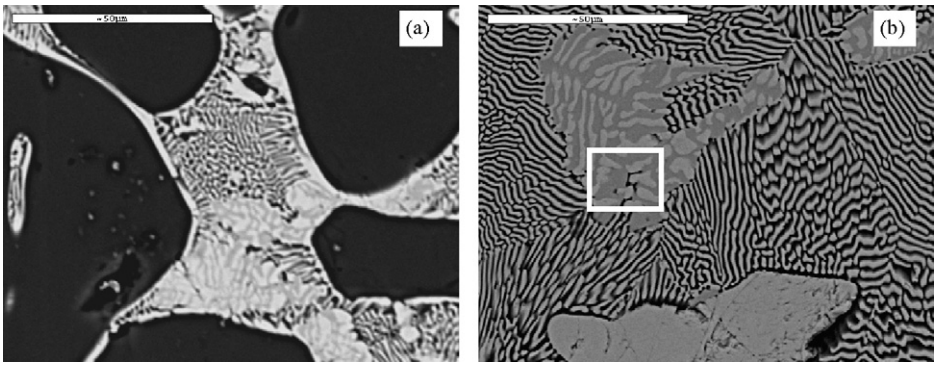

Fig. 4. The microstructures of Si–15Mn–9P (a); and Si–43Mn–26P (b) alloy.

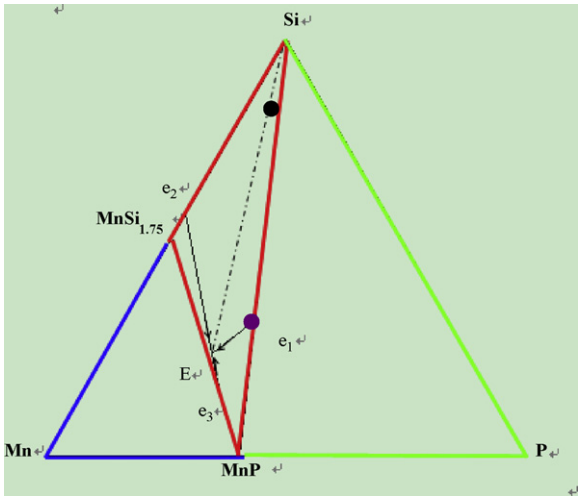

Fig. 5. The concentration triangle of Si–Mn–P ternary system divided into three parts by the lines between composition points of phases Si, $MnSi_{1.75-x}$ and MnP.

with the Si phase already existing in eutectic A, which leads to divorced structures appearing as the Si phase departing from MnP and $MnSi_{1.75-x}$ phases. Moreover, Si atoms can bring on the change of x in $MnSi_{1.75-x}$ without changing the crystal structure greatly since HMS have similar crystal structures. Only some dribs and drabs of Si phases could be seen in the eutectic B marked in rectangle, as shown in Fig. 4(b). Therefore, based on the discussions above, we can conclude that the eutectic B which appears to be made up of two phases is truly obtained through the ternary phase transformation from the liquid (i.e. the reaction: $L_2 \rightarrow (MnSi_{1.75-x} + Si + MnP)_E$ (the subscript E represents the eutectic crystals)).

However, the $(MnSi_{1.75-x} + MnP)$ in eutectic B as well take on similar to divorced structures but coupled growth as shown in Fig. 4. It is just because of the Si–15Mn–9P and Si–43Mn–26P whose initial composition is far away from the ternary eutectic point. Both the constituent positions of Si–15Mn–9P and Si–43Mn–26P in the concentration triangle are marked as black and purple points respectively shown in Fig. 5. So there is only a little residual liquid whose composition is near eutectic when the ternary eutectic temperature is reached. When the ternary eutectic transformation began, Si precipitate clinging to the eutectic A and MnP precipitates a lot as leading phase, and another phase $MnSi_{1.75-x}$ is left in the interdendritic region. Therefore, divorced eutectic structure tends to occur. So conclusion could be drawn from above is that the eutectic B is made up of Si phase separating from MnP and $MnSi_{1.75-x}$ which also appear divorced structures. The reaction $L_2 \rightarrow (MnSi_{1.75-x} + Si + MnP)_E$ is performed under the constant eutectic composition and temperature which also account for the fewer changes of the eutectic B's morphology. It can be also known that the Si–15Mn–9P and Si–43Mn–26P alloys could be distinguished by the primary phases mentioned above. The difference of the primary phase between the two alloys is attributed to their initial composition staying different primary regions.

Partial phase diagram of Mn–P–Si given at 800 °C for the concentration range from 0 to 50 at.% P has been illustrated [31]. However, solidification paths could not be obtained in the $MnSi_{1.75-x}$–Si–MnP composition region from that. Based on the phase constituents and solidification microstructures of Si–Mn–P alloy discussed above, it can be found that $MnSi_{1.75-x}$, Si and MnP phases could appear if the initial composition locates in the $MnSi_{1.75-x}$–Si–MnP composition region and there is no ternary phase. The solidification behavior of Si–Mn–P alloy could be predicted as follow if the initial composition locates $MnSi_{1.75-x}$–Si–MnP composition region with the Si as primary phase:

$$L \rightarrow L_1 + Si_p \rightarrow L_2 + Si_p$$

$$+ (Si + MnP)_E \rightarrow Si_p + (Si + MnP)_E + (MnSi_{1.75-x} + Si + MnP)_E$$

(ThesubscriptPrepresentstheprimaryparticles.)

While both $(Si + MnP)_E$ and $(MnSi_{1.75-x} + Si + MnP)_E$ exhibit binary eutectic structures because of the particularity for $(MnSi_{1.75-x} + Si + MnP)_E$ discussed in the above paragraphs.

4. Conclusion

1. Possible phases existing in some Si–Mn–P alloys were investigated. It is found that there is no ternary compound when the composition lies in the $MnSi_{1.75-x}$–Si–MnP region.
2. Microstructural formation of typical kinds of Si–Mn–P alloys was discussed. The primary Si or MnP phases are surrounded by (Si + MnP) binary eutectic structure with variety of morphologies and then by ternary eutectic $(Si + MnSi_{1.75-x} + MnP)$ with binary morphology due to divorced eutectic depended on the particularity of certain Si–Mn–P alloys.

Acknowledgments

This work was supported by a grant from National Science Fund for Distinguished Young Scholars of China (No. 50625101), Key Project of Science and Technology Research of Ministry of Education of China (No. 106103) and "Taishan Scholar" Construction Project for financial support of Shandong Province in China.

References

[1] X.F. Liu, M. Zuo, K. Jiang, C. Li, in: J. Hirsch, B. Skrotzki, G. Gottstein (Eds.), Aluminum Alloys, ICAA, Aachen Germany, 2008, pp. 115–120.
[2] M. Zuo, X.F. Liu, Q.Q. Sun, J. Mater. Sci. 44 (2009) 1952–1958.
[3] Y.P. Wu, S.J. Wang, H. Li, X.F. Liu, J. Alloys Compd. 477 (2009) 139–144.
[4] U. Hechta, L. Gránásyb, T. Pusztaib, B. Bo¨ttgera, M. Apela, V. Witusiewicz, Mater. Sci. Eng. R 46 (2004) 1–49.
[5] J. Dutkiewicz, T.B. Massalski, Metall. Trans. A 12A (1981) 773–778.
[6] A. Hawksworth, W.M. Rainforth, H. Jones, Scripta Mater. 39 (1998) 1371–1376.
[7] N. Wang, B. Wei, Mater. Sci. Eng. A 307 (2001) 80–90.
[8] C. Li, Y.Y. Wu, H. Li, X.F. Liu, J. Alloys Compd. 477 (2009) 212–216.
[9] G. Sauthoff, Intermetallics 8 (2000) 1101–1109.
[10] M. Jain, S.P. Gupta, Mater. Charact. 51 (2003) 243–257.
[11] O.M. Barabash, Yu.V. Milman, D.V. Miracle, Intermetallics 11 (2003) 953–962.
[12] O.P. Arora, Met. Trans. A 6A (1975) 1305–1309.
[13] O.N. Ii'nitskaya, Yu. B. Kuz'ma, Zh. Neorg. Khim. 27 (1982) 2713–2715.
[14] O.N. Ii'nitskaya, Yu. B. Kuz'ma, Poroshk. Metall. 10 (1992) 35–37.
[15] O.N. Ii'nitskaya, Yu. B. Kuz'ma, Zh. Neorg. Khim. 33 (1988) 2630–2633.
[16] O.N. Ii'nitskaya, Yu. B. Kuz'ma, Poroshk. Metall. 260 (1984) 56–57.
[17] X.F. Liu, X.J. Liu, X.Y. Liu, CN patent no. 1814840A, 2006.
[18] S. Teichert, S. Schwendlera, D.K. Sarkara, A. Mogilatenkoa, M. Falkea, J. Cryst. Growth 227–228 (2001) 882–887.
[19] Y. Miyazaki, D. Igarashi, K. Hayashi, T. Kajitani, Phys. Rev. B 78 (2008), pp. 214104-1–214104-8.
[20] D.K. Shi, Fundamentals of Materials Science, second ed., Mechanical Industry Press, Beijing, 2003.
[21] A. Karma, M. Plapp, JOM 4 (2004) 28–32.
[22] T.S. Lo, S. Dobler, M. Plapp, A. Karma, W. Kurz, Acta Mater. 51 (2003) 599–611.
[23] A. Parisi, M. Plapp, Acta Mater. 56 (2008) 1348–1357.
[24] L.Z. Cheng, Physical Chemistry, second ed., Shanghai Science and Technology Press, Shanghai, 1998.
[25] H. Jones, Mater. Lett. 26 (1996) 133–136.
[26] L. Katgerman, F. Dom, Mater. Sci. Eng. A 375–377 (2004) 1212–1216.
[27] K.A. Jackson, J.D. Hunt, Trans. Met. Soc. AIME 236 (1966) 1129–1142.
[28] Z. Chvoj, J. sestak, E. Fendrych, J. Therm. Anal. 43 (1995) 439–448.
[29] M.Y. Zhao, The Boundary Theory of the Phase Diagram and its Application, first ed., Science Press, Beijing, 2004.
[30] A.B. Gokhale, R. Abbaschlan, Bull. Alloy Phase Diagrams 11 (1990) 468–479.
[31] P. Villars, A. Prince, H. Okamoto, Handbook of Ternary Alloy Phase Diagrams, ASM International, New York, 1995, pp. 12416–12417.